FEBS Letters 580 (2006) 697–702

Characterization and inhibitor discovery of one novel malonyl-CoA: Acyl carrier protein transacylase (MCAT) from *Helicobacter pylori*

Weizhi Liu[a], Cong Han[a], Lihong Hu[a,b,*], Kaixian Chen[a], Xu Shen[a,b,*], Hualiang Jiang[a,b,*]

[a] *Drug Discovery and Design Center, State Key Laboratory of Drug Research, Shanghai Institute of Materia Medica, Shanghai Institutes for Biological Sciences, Graduate School of the Chinese Academy of Sciences, Chinese Academy of Sciences, 555 Zuchongzhi Road, Shanghai 201203, China*
[b] *School of Pharmacy, East China University of Science and Technology, Shanghai 200237, China*

Received 9 December 2005; revised 27 December 2005; accepted 27 December 2005

Available online 6 January 2006

Edited by Sandro Sonnino

Abstract **Type II fatty acid synthesis (FAS II) is an essential process for bacteria survival, and malonyl-CoA:acyl carrier protein transacylase (MCAT) is a key enzyme in FAS II pathway, which is responsible for transferring the malonyl group from malonyl-CoA to the holo-ACP by forming malonyl-ACP. In this work, we described the cloning, characterization and enzymatic inhibition of a new MCAT from *Helicobacter pylori* strain SS1 (*Hp*MCAT), and the gene sequence of *Hpfab*D was deposited in the GenBank database (Accession No. AY738332). Enzymatic characterization of *Hp*MCAT showed that the K_m value for malonyl-CoA was 21.01 ± 2.3 μM, and the thermal- and guanidinium hydrochloride-induced unfolding processes for *Hp*MCAT were quantitatively investigated by circular dichroism spectral analyses. Moreover, a natural product, corytuberine, was discovered to demonstrate inhibitory activity against *Hp*MCAT with IC_{50} value at 33.1 ± 3.29 μM. Further enzymatic assay results indicated that corytuberine inhibits *Hp*MCAT in an uncompetitive manner. To our knowledge, this is the firstly reported MCAT inhibitor to date. This current work is hoped to supply useful information for better understanding the MCAT features of *H. pylori* strain, and corytuberine might be used as a potential lead compound in the discovery of the antibacterial agents using *Hp*MCAT as target.**

Keywords: Fatty acid biosynthesis; Corytuberine; Unfolding; Antibacterial agents; Inhibition; *Helicobacter pylori*

1. Introduction

Fatty acid biosynthesis is an essential pathway for the survival of the organism since fatty acid is the major components of cell membrane and possesses important biological function. In nature, according to the enzyme involved in the pathway, fatty acid biosynthesis (FAS) is divided into two types, type I (FAS I) and type II (FAS II) [1–3]. In FAS I system, found in animals, the biosynthesis of fatty acid is catalyzed by a multi-enzyme, which is a single polypeptide with eight distinct domains. However, during the FAS II system, the reactions are carried out by a series of structurally dissociated enzymes as discovered in most of the bacteria [1,2]. Due to the large differences between these two FAS systems, the enzymes involved in the type II fatty acid biosynthesis have been developed as the attractive targets for the discovery of antibacterial agents [2].

Malonyl-CoA:acyl carrier protein transacylase (MCAT; FabD; EC2.3.1.39) is a vital enzyme within FAS II system, it catalyzes the transfer of a malonyl moiety from malonyl-CoA to holo-ACP, forming malonyl-ACP as the elongation substrate for the fatty acid biosynthesis [4–7]. The research has indicated that MCAT is essential for the completion of fatty acid synthesis, and the genetic inactivation of *fab*D is lethal in all pathogens [6,8,9]. Moreover, according to the recent report that the MCAT might participate in polyketide biosynthesis, it was regarded as the possible link between fatty acid and polyketide biosynthesis [10–12]. Therefore, MCAT has become a promising target in the discovery of antibacterial agents.

The solved crystal structures of MCAT from *Escherichia coli* (*Ec*MCAT) (PDB code:1MLA) and *Streptomyces coelicolor* (*Sc*MCAT) (PDB code:1NM2) indicated that both of these structures have similar structures, and the catalytic active site is composed of two subdomains [10,13,14]. One is made up of a short four-stranded parallel β-sheet and 12 helices, and the other contains a four-stranded anti-parallel β-sheet and two helices. The active residue (Ser 97) is reported to locate in the canyon of the two subdomains [10]. The overall structure of MCAT could be thus generally depicted as a typical α/β hydrolase model [10,13]. It is known that MCAT performs the transfer of malonyl group to the holo-ACP via the ping-pong bi–bi mechanism involving the His-Ser catalytic domain commonly contained in the serine-dependent acylhydrolases. The unusual feature for this mechanism is related to the existence of the stable MCAT-malonyl intermediate, while in most hydrolases, the formed possible enzyme-substrate intermediates might be rapidly broken down by the nucleophilic attack from the water molecules. It is reported that the formed stable MCAT-malonyl intermediate might be ascribed to the key residues of Arg117, Gln11, Gln63 in the structure of MCAT, which could interact with the malonate carboxylate group [2,10,13,15].

In recent years, bacterial diseases and antibiotic-resistant infections are globally increasing. They have become worldwide problems and governed the urgent needs for new drug design based on novel antibacterial targets [1,2,16]. *Helicobacter pylori* is a gram-negative clinic pathogenic bacterium, which is related to peptic ulcer and gastric cancer [17,18]. In this work,

*Corresponding authors. Tel./fax: +86 21 5080 6918 (X. Shen).
E-mail addresses: simmhulh@mail.shcnc.ac.cn (L. Hu), xshen@mail.shcnc.ac.cn (X. Shen), hljiang@mail.shcnc.ac.cn (H. Jiang).

Abbreviations: FAS, fatty acid biosynthesis; ACP, acyl carrier protein; MCAT, malonyl-CoA:acyl carrier protein transacylase; CD, circular dichroism; GndHCl, guanidinium hydrochloride; KDH, α-ketoglutarate dehydrogenase

0014-5793/$32.00
doi:10.1016/j.febslet.2005.12.085

we cloned and expressed the MCAT enzyme from *H. pylori* strain and some biochemical characterization was also performed against this enzyme. In addition, a natural product, corytuberine, was discovered to demonstrate inhibitory activity against *Hp*MCAT in an uncompetitive manner. Corytuberine is a kind of alkaloid with multi-pharmacological activity. To our knowledge, this is the firstly reported MCAT inhibitor to date. Our work is hoped to supply useful information for better understanding the MCAT features of *H. pylori* strain, and the inhibitor corytuberine might be used as a potential lead compound in the discovery of antibacterial agents.

2. Materials and methods

2.1. Materials and strains

H. pylori strain SS1 was obtained from our institute. *E. coli* host strain M15 was purchased from Qiagen. The natural product corytuberine (Fig. 1) was from a chemical library containing 5000 compounds established in our lab. All other chemicals were of reagent grade or ultra-pure quality, and commercially available.

2.2. Cloning of the *fabD* gene from *H. pylori* (*HpfabD*)

Based on the genome sequences of *H. pylori* strains 26695 and J99 (GenBank Accession Nos. NC_000915 and NC_000921), two polymerase chain reaction (PCR) primers (forward: 5′-CAAAATCCACGCCAAACAATTCTAG-3′ and reverse: 5′-CTTTAATGGTTTCTAAACAAAACTAAGGGC-3′) were designed to amplify the corresponding region containing *fab*D gene from the chromosome of *H. pylori* strain SS1. The genomic DNA of *H. pylori* strain SS1 as a template was prepared by using Genomic DNA Extraction Kit (Sangon). The reaction was performed for 30 cycles: 45 s at 94 °C, 45 s at 53 °C, and 1.5 min at 72 °C. The amplified DNA segment was purified and subjected to nucleotide sequencing. According to the sequencing result, a pair of primers (sense: 5′-TTTGGATCCATGCAATACGCGCTATTA-3′, and antisense: 5′-GGGGAAGCTTTCACACGTATTCTAA-3′) was synthesized to amplify the *fab*D gene from *H. pylori* strain SS1. The following protocol was conducted for amplification: 30 s at 94 °C, 30 s at 50 °C, and 1 min at 72 °C, 30 cycles. The PCR products were digested with restriction endonuclease *Bam*HI and *Hin*dIII (Fermentas), and ligated into a prokaryotic expression vector pQE30 (Qiagen) to produce the recombinant plasmid pQE30-*Hpfab*D that contains an N-terminal six-histidine tag for purification purpose. After the recombinant clone pQE30-*Hpfab*D was sequenced, the nucleotide sequence of *fab*D gene from *H. pylori* strain SS1 was submitted to GenBank database under the Accession No. AY738332.

2.3. Expression and purification of *Hp*MCAT

pQE30-*Hpfab*D was transformed into *E. coli* strain M15 growing in LB media supplemented with 100 μg/ml of ampicillin and 50 μg/ml of kanamycin at 37 °C. When OD_{600} reached 0.8, the culture was induced by 0.4 mM isopropyl-β-D-thiogalasctopyranoside and incubated at 37 °C for an additional 6 h. The cells were harvested by centrifugation at 6000 × *g* for 15 min at 4 °C and suspended in buffer A (20 mM Tris–HCl, pH 8.0, 500 mM NaCl, and 5 mM imidazole). After sonication treatment on ice, the mixture yielded a clear supernatant by centrifugation at 16000 × *g* for 45 min at 4 °C, which was loaded onto a column with Ni-NTA resin (Qiagen) pre-equilibrated in buffer A. The column was washed with buffer B (20 mM Tris–HCl, pH 8.0, 500 mM NaCl, and 40 mM imidazole) for several times and eluted with buffer C (20 mM Tris–HCl, pH 8.0, 500 mM NaCl, and 500 mM imidazole). The proper concentration of *Hp*MCAT was obtained by ultra filtration using Amicon centrifugal device and determined by measuring the absorbance at 280 nm with the extinction coefficient of 19785 L/mol/cm.

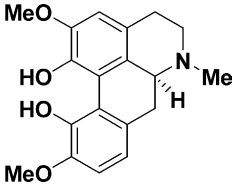

Fig. 1. Chemical structure of corytuberine, the identified inhibitor against *Hp*MCAT.

2.4. Circular dichroism (CD) technique based unfolding analysis

All the CD spectral investigations for *Hp*MCAT were carried out using a JASCO J-810 spectropolarimeter under constant nitrogen flow. The *Hp*MCAT concentration was 0.3 mg/ml in 50 mM, pH 6.8, phosphate buffer for far-UV (190–250 nm) assay using 1 mm quartz cell.

To determine the temperature-induced unfolding of *Hp*MCAT, the change of ellipticity at 220 nm was recorded at a scan speed of 0.2 °C/min from 20 to 90 °C. Since the buffer solution showed no changes with the increase of temperature, the potential buffer-caused effect could be neglected during data analysis.

During the guanidinium hydrochloride (GndHCl)-induced unfolding experiment, the spectra were obtained with 2-h incubation at room temperature including the supplement of corresponding concentration of GndHCl. Experimental data were corrected by subtracting the blank obtained under the same conditions in the absence of protein sample.

The standard free energy change of GndHCl-induced unfolding process (ΔG) for *Hp*MCAT was obtained in terms of the typical two state transition mechanism. In this unfolding reaction, the equilibrium constant (K_u) could be expressed as follows:

$$K_u = (1 - F_{app})/F_{app}, \quad F_{app} = (\theta - \theta_U)/(\theta_N - \theta_U), \tag{1}$$

where θ is the observed ellipticity value in 220 nm of *Hp*MCAT at a given GndHCl concentration, θ_U and θ_N are the ellipticity values when *Hp*MCAT is completely unfolded and in native state, respectively. The calculation of the standard free energy of GndHCl-induced unfolding (ΔG) is obtained according to the following equation:

$$\Delta G = -RT \ln(K_u), \tag{2}$$

where R is the gas constant, T is the absolute temperature. ΔG is then fitted to the linear regression by the concentration of GndHCl (C) using the following equation [19]:

$$\Delta G = mC + \Delta G^{H_2O}, \tag{3}$$

where the slope (m) is the cooperative index, which reflects the ability of the denaturant to unfold a protein. ΔG^{H_2O} could be calculated by linear extrapolation, which represents the structural stability of *Hp*MCAT in buffer. At the midpoint concentration of GndHCl (C_m), ΔG is zero, C_m could be thus calculated according to Eq. (3).

2.5. Enzyme activity assay

The enzymatic activity of *Hp*MCAT was measured by using the α-ketoglutarate dehydrogenase (KDH)-coupled assay system [20]. In this system, the coenzyme A (CoASH) generated by *Hp*MCAT is the substrate for the KDH-dependent reaction, which is accompanied by the reduction of NAD^+ to NADH. The rate of NAD^+ is detected as a change in fluorescence using a 96-well plate system (Tecan GENios reader) with an excitation wavelength at 340 nm and the emission wavelength at 465 nm. The assay solution contained 50 mM phosphate buffer (pH 6.8), 1 mM EDTA, 1 mM DTT, 2 mM α-ketoglutaric acid, 0.25 mM NAD^+, 0.2 mM TPP, 1 μg *Hp*MCAT, 10 μM acyl carrier protein (ACP), 5 mU/100 μl KDH, and 25 μM malonyl-CoA. The reaction was formed in the following order with 50 μl *Hp*MCAT solution, 25 μl ACP/KDH mix, and then 25 μl malonyl-CoA to initiate the reaction. The change of NADH fluorescence was recorded for 30 min at 30 °C.

The concentrations of malonyl-CoA were individually varied as required to obtain the K_m value for *Hp*MCAT toward malonyl-CoA. The influence of temperature on the enzymatic activity was determined from 20 to 50 °C.

For the enzyme inhibition studies, the test compound dissolved in 1% DMSO was pre-incubated with *Hp*MCAT at 30 °C for 1 h before the reaction was started. In considering that the inhibitor might interfere with the activity of KDH, the counter-screen was performed against KDH to identify its effect on the KDH activity [20].

3. Results and discussion

3.1. fabD gene sequence analysis

In the current work, the *fab*D gene from *H. pylori* strain SS1 (*Hpfab*D) was successfully cloned based on the available genome sequences of *H. pylori* strains 26695 and J99, and the recombinant expression plasmid pQE30-*Hpfab*D was generated by inserting the amplified *fab*D fragment into the vector pQE30. The *Hpfab*D gene was a 930 bp fragment including the stop codon.

Fig. 2 showed the amino acid sequence alignment of *Hp*MCAT with other MCATs from several other model organisms by Clustal W (www.ebi.ac.uk/clustalw). It was found that *Hp*MCAT shared 32% identity and 53% similarity with MCAT of *E. coli* (*Ec*MCAT) in amino acid sequence. In addition, two highly conserved motifs (GHSXH, PGQGXQ) and other conserved residues were observed. According to the previous reports involving the crystallographic and catalytic mechanism analyses for MCAT, MCAT performs the transfer of malonyl to holo-ACP including two reactions [4,7,10]. Firstly, the MCAT binds the malonyl-CoA substrate to form a stable tetrahedral malonyl-MCAT intermediate, the holo-ACP could then dock on the surface of the intermediate by hydrophobic interaction [10]. Thus, MCAT enzyme was generally considered to contain at least two active sites, the malonyl-CoA binding site and the holo-ACP binding site. It is suggested that the two highly conserved motifs and residues might be related to the active sites formation [2,10,13].

3.2. Purification and characterization of HpMCAT

*Hp*MCAT could be successfully expressed as a fusion protein with an N-terminal 6× His tag. It could be purified by a one-step purification protocol judged from SDS–PAGE (Fig. 3A), and Electron-spray ionization mass spectrometry yielded a molecular mass about 35755 Da (Supplementary material), in good agreement with the calculated molecular mass according to the amino acids compositions.

The far-UV CD spectrum of native *Hp*MCAT in, pH 6.8, 50 mM phosphate buffer at 25 °C revealed two negative peaks at 209 and 220 nm, implying that this protein contains a significant amount of α-helix as shown in Fig. 3B [21]. According to the JASCO secondary structure estimation software, in the native state of *Hp*MCAT, its α-helix is about 64.2%, which is higher than that obtained from *Ec*MCAT based on its crystal structure (49.5%, α-helix) [13].

3.3. Enzymatic kinetics analysis

It is known that *Hp*MCAT catalyzes the transfer of a malonyl moiety from malonyl-CoA to the free thiol of phosphopantetheine arm of ACP using the ping-pong mechanism [10,20], which could be depicted in the reactions as follows:

$$\text{Malonyl-CoA} + \text{holo-ACP} \leftrightarrow \text{malonyl-ACP} + \text{CoASH} \quad (4)$$

$$\text{CoASH} + \text{NAD}^+ + \alpha\text{-ketoglutarate} \rightarrow \text{succinyl-CoA} + \text{NADH} + \text{CO}_2 \quad (5)$$

```
E.coli              -MTQFAFVFPGQGSQTVGMLADMAASYPIVEETFAEASAALGYDLWALTQQGPAEELNKT 59
P.aeruginosa        MSASLAFVFPGQGSQSLGMLAELGAQQALVRDTFAEASEALGYDLWALVQNGPEERLNQT 60
S.coelicolor        ---MLVLVAPGQGAQTPGFLTDWLALPG-AADRVAAWSDAIGLDLAHFGTKADADEIRDT 56
H.pylori            --MQYALLFPGQGSQCIGMGKSFYEGHTLAKELFERASNALKVDMKKTLFE-ENELLKES 57
                        .:: ****:*  *:  .       . : .   * *:  *:      :   : :.. :

E.coli              WQTQPALLTASVALYRVWQQHG---------GKAPAMMAGHSLGEYSALVCAGVIDFADAV 111
P.aeruginosa        DKTQPAILTVSIALWRLWLAEG---------GARPAFVAGHSLGEYSALVAAESLAFADAV 112
S.coelicolor        SVAQPLLVAAGILSAAALGTQTSVADATGPGFTPGAVAGHSVGEITAAVFAGVLDDTAAL 116
H.pylori            AYTQPAIYLVSYIAYQLLNKQANG-------GLKPVFALGHSLGEVSAVSLSGALDFEKAL 111
                      :** :  ..          .          *  *    ***:** :*   :  :    *:

E.coli              RLVEMRGKFMQEAVPEGTGAMAAIIGLDDASIGKACEEAAEGQVVSPVNFNSPGQVVIAG 171
P.aeruginosa        KLVERRGQLMQQAVPAGQGGMAAILGLEDADVLAACAEAAQGEVVSAVNFNAPGQVVIAG 172
S.coelicolor        SLVRRRGLAMAEAAAVTETGMSALLG-GDPEVSVAHLERLG---LTPANVNGAGQIVAAG 172
H.pylori            KLTHQRGKMMQEACANKDASMMVVLGVSEESLLSLCQRTKN---VWCANFNGGMQVVLAG 168
                     *.. **  * :* .    .* . ::*  : . :      .       :  .*.*.  *:* **

E.coli              HKEAVERAGAACKAAGAKRALPLPVSVPSHCALMKPAADKLAVELAKITFNAPTVPVVNN 231
P.aeruginosa        AAAAVERAIEACKARGAKRAVALPVSVPSHCELMRPAAEQFAASVESLQWQAPKISLVQN 232
S.coelicolor        TMEQLA-ALNEDKPEGVRKVVPLKVAGAFHTRHMAPAVDKLAEAAKALTPADPKVTYVSN 231
H.pylori            VKDDLKALEPTLKEMGAKRVVFLEMSVASHCPFLEPMIFKFQELLEKSLKDKFHFEIISN 228
                         :         *  *. ::. : * :: .  *    : *    ::               .   :.*

E.coli              VDVKCETNGDAIRDALVRQLYNPVQWTKSVEYMAAQGVEHLYEVGPGKVLTGLTKRIVDT 291
P.aeruginosa        VSAAVPADLDTLRRDLLAQLYSPVRWVESIQLLAEKGVTELVECGPGKVLAGLNRRCAKG 292
S.coelicolor        KDGRAVASGTEVLDRLVGQVANPVRWDLCMETFKELGVTAIIEVCPGGTLTGLAKRALPG 291
H.pylori            ATNEAYHNKAKAVELLSLQLTQPVRYQDCVKSNNDR-VDIFFELGCGSVLKGLNKRLSN- 286
                           .         *  *: .**::  .::       *  : *   * .* ** :*

E.coli              LTASALNEPSAMAAALEL-------- 309
P.aeruginosa        INTHGLDGVEAFAATRAALA------ 312
S.coelicolor        VKTLALKTPDDLDAARELVAEHTQA 316
H.pylori            KPTISVGDNKGLDEAIEFLEEYV-- 309
                      : :  :  :  :  :
```

Fig. 2. Multiple alignment of MCAT sequences from different species. *Escherichia coli* (*E. coli*), *Pseudomonas aeruginosa* (*P. aeruginosa*), *Streptomyces coelicolor* (*S. coelicolor*), *Helicobacter pylori* (*H. pylori*). The strictly conserved residues are marked with asterisk "*". The conserved substitutions are represented as ":", and "." means the semi-conserved substitutions. Alignment was performed using Clustal W at http://www.ebi.ac.uk/clustal/index.html website.

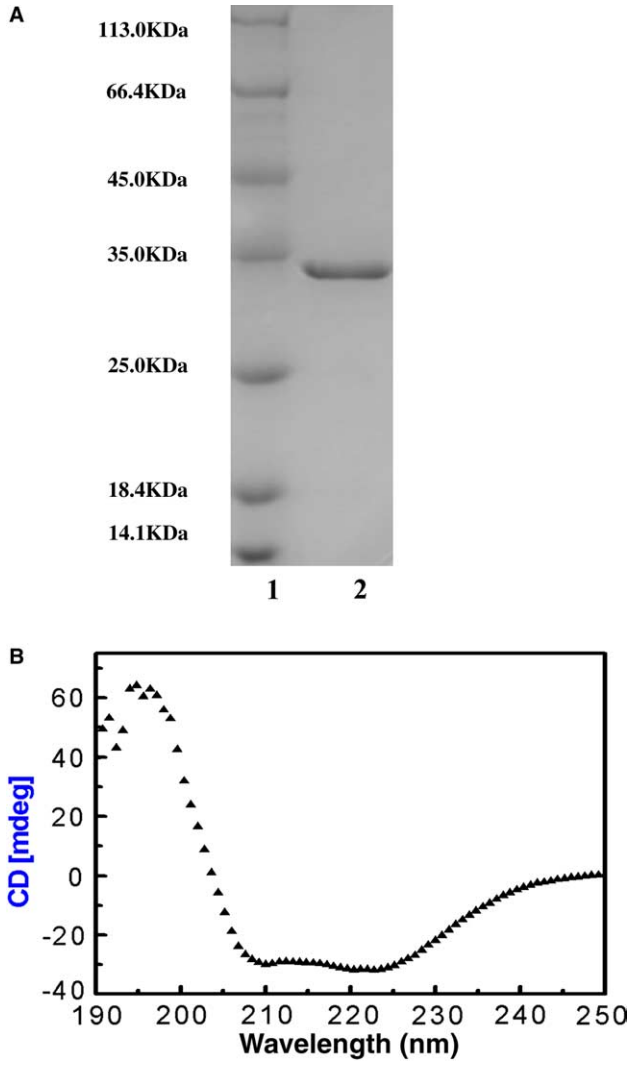

Fig. 3. Characterization of the purified *Hp*MCAT. (A) SDS–PAGE in 5%, pH 6.8, stacking gel and 10%, pH 8.8, separating gel. Lane 1, molecular mass marker; lane 2, *Hp*MCAT. (B) Far-UV CD spectra of *Hp*MCAT.

The rate of NAD^+ reduction to NADH could be recorded as a change in fluorescence. The enzymatic results thus showed that *Hp*MCAT was active with K_m at 21.01 ± 2.3 μM toward the malonyl-CoA as indicated in Fig. 4, similar to that of *Ec*MCAT [20], and smaller than that of *Sc*MCAT [22]. In addition, the *Hp*MCAT enzyme showed the highest enzymatic activity at 30 °C. When the temperature was increased to 50 °C, the enzyme could only possess about 20% activity as shown in Fig. 5.

3.4. Enzyme unfolding analyses

To determine the influence of temperature on the stability of *Hp*MCAT, the thermal-induced unfolding experiment was carried out using CD technique. As shown in Fig. 6A, *Hp*MCAT began to lose its secondary structure at 50 °C, and its secondary structure was totally destroyed when the temperature was raised to 70 °C. However, it is noticed that the enzymatic activity of *Hp*MCAT was mostly vanished even when the temperature was raised to 45 °C as indicated in Fig. 5. This result implied that the secondary structure of *Hp*MCAT seems to be more thermostable in comparison with its three-dimensional structure.

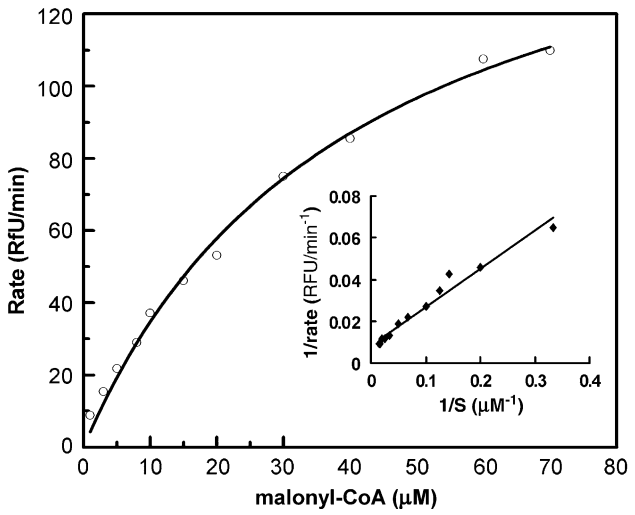

Fig. 4. Kinetic analysis of *Hp*MCAT toward malonyl-CoA using the fluorometric coupled enzyme assay. The assay was performed as described in Section 2. The K_m for *Hp*MCAT toward malonyl-CoA value was obtained upon the data analysis by double reciprocal plot.

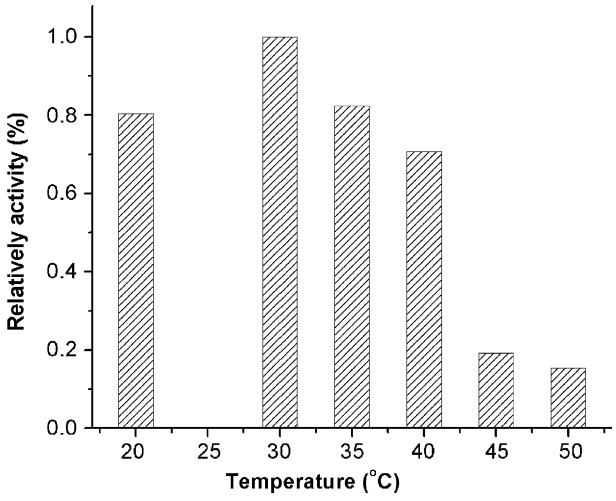

Fig. 5. Effect of temperature on the *Hp*MCAT enzymatic activity.

In order to further gain insights into the thermal-induced unfolding process, the thermodynamic parameters for *Hp*MCAT were quantitatively analyzed [23,24]. As shown in Fig. 6A, the change of ellipticity at 220 nm with the increase of temperature demonstrates that the thermal-induced unfolding process of *Hp*MCAT is cooperative and follows a typical two-state pattern. The apparent activation energy (E_a) of the transition of *Hp*MCAT could be obtained according to the following equation [24]:

$$\ln(\ln(1/F_{app})) = E_a/R(1/T_m - 1/T), \quad (6)$$

where F_{app} is defined as the fraction of native protein at the corresponding temperature. F_{app} is equal to the $(\theta - \theta_U)/(\theta_N - \theta_U)$, θ is the observed ellipticity value in 220 nm of *Hp*MCAT at a given temperature, θ_U and θ_N are the ellipticity values when the *Hp*MCAT is completely unfolded and in native state, respectively. T_m is the temperature at which the maximum of the heat capacity curve happened. The plot of

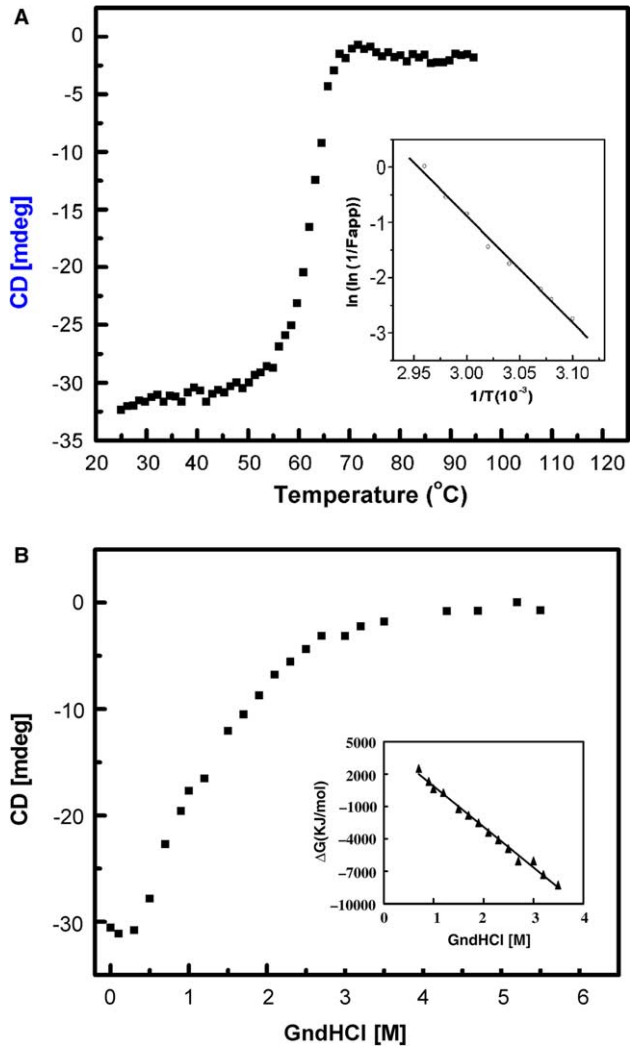

Fig. 6. Unfolding analysis of *Hp*MCAT determined by far-UV CD spectra. (A) Thermal-induced unfolding. The ellipticity value at 220 nm of *Hp*MCAT (0.3 mg/ml) was recorded from 20 to 90 °C with the scan rate of 2 °C/min. The inset shows the relationship between the $\ln(\ln(1/F_{app}))$ and $1/T$ (Eq. (6)). (B) GndHCl-induced unfolding. The ellipticity value at 220 nm of *Hp*MCAT (0.3 mg/ml) was monitored at the function of GndHCl at 25 °C. The inset reveals the linear relationship between the free energy (ΔG) and the GndHCl concentrations.

$\ln(\ln(1/F_{app}))$ versus $1/T$ showed that they have linear correlation (Fig. 6A, inset). According to Eq. (6), at pH 6.8 the apparent activation energy (E_a) of *Hp*MCAT and T_m were estimated to be 160.1 ± 6.6 (kJ/mol) and 65.5 ± 2.5 °C, respectively.

It is known that GndHCl is the most commonly used ion-denaturant in the evaluation of protein stability [24]. To investigate the effect of detergent on the stability of *Hp*MCAT, GndHCl-induced unfolding assay for *Hp*MCAT was performed using CD technique. As shown in Fig. 6B, a single transition was observed with increasing GndHCl concentrations from 0.7 to 4 M. On the basis of the experimental data, the GndHCl-induced unfolding could be also described in a two-state pathway, similar to the thermal-induced unfolding nature as indicated in Fig. 6. According to Eqs. (2) and (3), the C_m value (1.3 ± 0.2 M GndHCl), m value (3.58 ± 0.5 kJ/mol) and ΔG^{H_2O} of unfolding (4.67 ± 0.7 kJ/mol) could be obtained.

3.5. Corytuberine is an uncompetitive inhibitor of HpMCAT

It is known that MCAT could catalyze the formation of malonyl-ACP, which is a key substrate for the biosynthesis of fatty acid in bacteria (FAS II). Accordingly, MCAT has been developed as a promising drug target for antibacterial agent discovery. In the current work, we have constructed the high-throughput screening (HTS) assay for the discovery of the potent small molecular inhibitors against *Hp*MCAT based on our natural products library. Up to now, several inhibitors against some other enzymes involved in FAS II process have been investigated. For example, triclosan and diazaborine showed inhibitory activity against the enoyl-ACP reductase (FabI) [25–27]. However, no inhibitor has been reported against MCAT enzyme [1,2,28]. In the current work, we firstly discovered a small natural compound, corytuberine (Fig. 1), which demonstrated evidently enzymatic inhibitory activity against *Hp*MCAT and no effects on KDH (data not shown) during the enzymatic inhibition assay. This result thereby indicates that corytuberine is a potent inhibitor against *Hp*MCAT. The IC_{50} value for this inhibition was evaluated as 33.1 ± 3.29 μM (Fig. 7, inset) by fitting the inhibition data to a dose-dependent curve using a logistic derivative equation.

To further elucidate the inhibition mode of corytuberine against *Hp*MCAT, the enzymatic kinetic studies were carried out according to the published methods [20,29]. The results showed that with malonyl-CoA as the variable substrate, corytuberine gave the uncompetitive inhibition pattern with respect to malonyl-CoA according to the double reciprocal plot as shown in Fig. 7 and Table 1.

In conclusion, we described the clone and expression of a novel MCAT from *H. pylori* (*Hp*MCAT), the sequence alignment

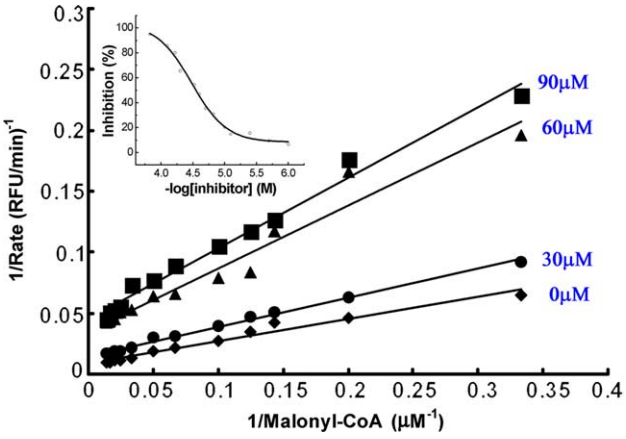

Fig. 7. Kinetic analysis of the inhibitory activity for corytuberine against *Hp*MCAT. The reaction was performed under the conditions as described in Section 2 in the presence of different concentrations of corytuberine (0, 30, 60, 90 μM) at a range of malonyl-CoA concentrations. The data were analyzed by double reciprocal plot. (Inset: Dose–response curves of enzyme inhibition.)

Table 1
Comparison of K_m and V_m of *Hp*MCAT toward malonyl-CoA at different inhibitor (corytuberine) concentrations

Inhibitor concentration (μM)	0	30	60	90
K_m (μM)	21.01	16.38	14.65	12.76
V_m (RFU/min)	114.9	68.5	28.41	22.03

demonstrated that MCAT is a conserved enzyme among different species. The biochemical characterization and stability investigation of *Hp*MCAT were carried out by CD spectral assay, which provided some useful insights into the understanding of the *Hp*MCAT enzyme. Furthermore, a small molecular natural product, corytuberine, was discovered as a potent inhibitor against *Hp*MCAT. To our knowledge, this is the first MCAT inhibitor to date. Further enzymatic dynamic assay indicated that corytuberine inhibits *Hp*MCAT in an uncompetitive manner. This current work is hoped to supply useful information for better understanding the MCAT features of *H. pylori* strain and further providing possible hints in the discovery of the antibacterial compounds using *Hp*MCAT as target. The inhibitor, corytuberine, might be used as a potential lead compound in the discovery of antibacterial agents.

Acknowledgments: This work was supported by the State Key Program of Basic Research of China (Grants 2002CB512807 and 2004CB58905), the National Natural Science Foundation of China (Grants 30525024, 20372069, and 20472095), Shanghai Basic Research Project from the Shanghai Science and Technology Commission (Grants 03DZ19228, 054319908, and 03DZ19212).

Appendix A. Supplementary data

Supplementary data associated with this article can be found, in the online version, at doi:10.1016/j.febslet.2005.12.085.

References

[1] Campbell, J.W. and Cronan Jr., J.E. (2001) Bacterial fatty acid biosynthesis: targets for antibacterial drug discovery. Annu. Rev. Microbiol. 55, 305–332.
[2] White, S.W., Zheng, J., Zhang, Y.M. and Rock, C.O. (2005) The structure biology of typeII fatty acid biosynthesis. Annu. Rev. Biochem. 74, 791–831.
[3] Magnuson, K., Jackowski, S., Rock, C.O. and Cronan Jr., J.E. (1993) Regulation of fatty acid biosynthesis in *Escherichia coli*. Microbiol. Rev. 57, 522–542.
[4] Ruch, F.E. and Vagelos, P.R. (1973) The isolation and general properties of *Escherichia coli* malonyl coenzyme A-acyl carrier protein transacylase. J. Biol. Chem. 248, 8086–8094.
[5] Williamson, I.P. and Wakil, S.J. (1966) Studies on the mechanism of fatty acid synthesis. J. Biol. Chem. 241, 2326–2332.
[6] Kutchma, A.J., Hoang, T.T. and Schweizer, H.P. (1999) Characterization of a *Pseudomonas aeruginosa* fatty acid biosynthetic gene cluster: purification of acyl carrier protein (ACP) and malonyl-Coenzyme A:ACP transacylase (FabD). J. Bacteriol. 181, 5498–5504.
[7] Verwoert, G.S., Verbree, E.C., Linden, K.H., Nijkamp, H.J. and Stuitje, A.R. (1992) Cloning, nucleotide sequence and expression of the *Escherichia coli* fabD gene, encoding malonyl coenzyme a-acyl carrier protein transacylase. J. Bacteriol. 174, 2851–2857.
[8] Harder, M.E., Ladenson, R.C., Schimmel, S.D. and Silbert, D.F. (1974) Mutants of *Escherichia coli* with temperature-sensitive malonyl coenzyme a-Acyl carrier protein transacylase. J. Biol. Chem. 249, 7468–7475.
[9] Verwoert, I.I., Verhagen, E.F., Van der Linden, K.H., Verbree, E.C., Nijkamp, H.J. and Stuitjie, A.R. (1994) Molecular characterization of an *Escherichia coli* mutant with a temperature-sensitive malonyl-coenzyme A-acyl carrier protein transacylase. FEBS Lett. 348, 311–316.
[10] Keatinge-Clay, A.T., Shelat, A.A., Savage, D.F., Tsai, S.C., Miercke, L.J., O'Connell, J.D., Khosla, C. and Stroud, R.M. (2003) Catalysis, specificity, and ACP docking site of *Streptomyces coelicolor* malonyl-CoA:ACP transacylase. Structure 11, 147–154.
[11] Summers, R.G., Ali, A., Shen, B., Wessel, W.A. and Hutchinson, C.R. (1995) Malonyl-Coenzyme A:acyl carrier protein acyltransferase of *Streptomyces glaucescens*: a possible link between fatty acid and polyketide biosynthesis. Biochemistry 34, 9389–9402.
[12] Arthur, C.J., Szafranska, A., Evans, S.E., Findlow, S.C., Burston, S.G., Owen, P., Clark-Lewis, I., Simpson, T.J., Crosby, J. and Crump, M.P. (2005) Self-malonylation is an intrisinsic property of a chemically synthesized typeII polyketide synthase acyl carrier protein. Biochemistry 44, 15414–15421.
[13] Serre, L., Verbree, E.C., Dauter, Z., Stuitje, A.R. and Derewenda, Z.S. (1995) The *Escherichia coli* malonyl-CoA:acyl carrier protein transacylase at 1.5-Å resolution. J. Biol. Chem. 270, 12961–12964.
[14] Serre, L., Swenson, L., Green, R., Wei, Y., Verwoert, I.I.G.S., Verbree, E.C., Stuitje, A.R. and Derewenda, Z.S. (1994) Crystallization of the malonyl coenzyme A-Acyl carrier protein transacylase from *Escherichia coli*. J. Mol. Biol. 242, 99–102.
[15] Ruch, F.E. and Vagelos, P.R. (1973) Characterization of a malonyl-enzyme intermediate and identification of the malonyl binding site in malonyl coenzyme A-acyl carrier protein transacylase of *Escherichia coli*. J. Biol. Chem. 248, 8095–8106.
[16] Kodali, S., Galgoci, A., Young, K., Painter, R., Sliver, L.L., Herath, K.B., Singh, S.B., Cully, D., Barrett, J.F., Schmatz, D. and Wang, J. (2005) Determination of selectivity and efficacy of fatty acid synthesis inhibitors. J. Biol. Chem. 280, 1669–1677.
[17] Schilling, C.H., Covert, M.W., Famili, I., Church, G.M., Edwards, J.S. and Palsson, B.O. (2002) Genome-scale metabolic model of *Helicobacter pylori* 26695. J. Bacteriol. 184, 4582–4593.
[18] Liu, W.Z., Luo, C., Han, C., Peng, S.Y., Yang, Y.M., Yue, J.M., Shen, X. and Jiang, H.L. (2005) A new beta-hydroxyacyl-acyl carrier protein dehydratase (FabZ) from *Helicobacter pylori*: molecular cloning, enzymatic characterization, and structural modeling. Biochem. Biophys. Res. Commun. 333, 1078–1086.
[19] Chedad, A. and Van Deal, H. (2004) Kinetics of folding and unfolding of goat alpha-lactalbumin. Proteins 57, 345–356.
[20] Molnos, J., Gardiner, R., Dale, G.E. and Lange, R. (2003) A continuous coupled enzyme assay for bacterial malonyl-CoA:acyl carrier protein transacylase (FabD). Anal. Biochem. 319, 171–176.
[21] Greenfield, N.J. (1996) Methods to estimate the conformation of proteins and polypeptides from circular dichroism data. Anal. Biochem. 235, 1–10.
[22] Szafranska, A.E., Hitchman, T.S., Cox, R.J., Crosby, J. and Simpson, T. (2002) Kinetic and mechanistic analysis of the malonyl CoA:ACP transacylase from *Streptomyces coelicolor* indicates a single catalytically competent Serine nucleophile at the active site. Biochemistry 41, 1421–1427.
[23] Tello-Solis, S.R. and Romero-Garcia, B. (2001) Thermal denaturation of porcine pepsin:a study by circular dichroism. Int. J. Biol. Macromol. 28, 129–133.
[24] Yu, C.Y., Gui, C.S., Luo, H., Chen, L.L., Zhang, L., Yu, H., Yang, S., Jiang, W.H., Shen, J.H., Shen, X. and Jiang, H.L. (2005) Folding of the SARS coronavirus spike glycoprotein immunological fragment (SARS_S1b): thermodynamic and kinetic investigation correlating with three-dimensional structural modeling. Biochemistry 44, 1453–1463.
[25] Heath, R.J., White, S.W. and Rock, C.O. (2002) Inhibitors of fatty acid synthesis as antimicrobial chemotherapeutics. Appl. Microbiol. Biotechnol. 58, 695–703.
[26] Heath, R.J., Rubin, J.R., Holland, D.R., Zhang, E., Snow, M.E. and Rock, C.O. (1999) Mechanism of triclosan inhibition of bacterial fatty acid synthesis. J. Biol. Chem. 274, 11110–11114.
[27] Stewart, M.J., Parikh, S., Xiao, G., Tonge, P.J. and Kisker, C. (1999) Structural basis and mechanism of enoyl reductase inhibition by triclosan. J. Mol. Biol. 290, 859–865.
[28] Lu, J.Z., Lee, P.J., Waters, N.C. and Prigge, S.T. (2005) Fatty acid synthesis as a target for antimalarial drug discovery. Comb. Chem. High Throughput Screen. 8, 15–26.
[29] Wiesmann, C., Barr, K.J., Kung, J., Zhu, J., Erlanson, D.A., Shen, W., Fahr, B.J., Zhong, M., Taylor, L., Randal, M., McDowell, R.S. and Hansen, S.K. (2004) Allosteric inhibition of protein tyrosine phosphatase 1B. Nat. Struct. Mol. Biol. 11, 730–737.